# Supramolecular core-shell heterostructures with controllable multi-color-emitting properties

Hongyang Zhang,[a,b] Yilong Lei,[a,b] Haitao Wang,[b] and Wai-Yeung Wong*[a,b]

**Herein, we report novel supermolecular heterojunctions with six kinds of multi-layer core-shell microstructures, which consist of up to three CT complex components that realize the programmable fabrication with defined luminescent CT domains and controllable multi-color-emitting properties. A stepwise seeded-growth route was designed using these CT cocrystals as seed and growing units during the process of fabrication where a solution-epitaxy growth would occur based on their perfect lattice matching. This rational multi-step synthetic route furnishes a new insight to develop and construct more sophisticated organic heterogeneous materials.**

## 1. Introduction

Organic heterojunctions comprising dissimilar constituent materials have been demonstrated to exhibit a wide range of promising applications in functional optoelectronic devices, such as organic field-effect transistors (OFETs),[1,2,3,4,5] organic light-emitting diodes (OLEDs)[6,7,8] and organic solar cells (OSCs).[9,10,11,12] Although great successes have been made, almost all of the related works on organic heterojunctions focused on their amorphous thin-film forms.[13] In contrast, the successful synthesis of crystalline organic heterostructured nanomaterials with precisely distributed domains still remains a big problem owing to the great difficulty of rational selection of each material and their dynamic assembly control. Meanwhile, it is also reasonable that the nano or microscale organic heterojunctions exhibit superior properties due to the creation of unique interfacial structures.[14,15] As a result, efficient energy and electron transfer would occur across the interfaces between different domains, leading to novel and/or improved photonic and electronic performances, like multi-color fluorescent barcodes[15,16,17] and ambipolar p-n diodes.[14,18,19] For instance, phosphorescent heterostructured nanorods that consist of binary metallophosphors were constructed into high-quality crystals through the stepwise growth method, in which the process of coassembly is able to be visualized and the prepared heterostructured nanorods display multicolor phosphorescent properities with advanced optical signal processing application.[17] Moreover, the linear heterojunctions composed of two- and three-block nanotubular segments have been elaborately designed and developed by the seed-induced stepwise assembly of two structurally matched graphene-like molecules with dissimilar semiconducting properties.[20] The generated interfaces between the two blocks favour charge-transfer (CT) from one p-type molecule to another n-type molecule and thus suppress charge recombination. It should be noted that specially designed molecular pairs with well-matched structures are necessary to realize the complex configurations.

From the viewpoint of crystal engineering, a cocrystal strategy formed by simply integrating together two common π-conjugated materials may be a promising alternative, avoiding complicated multistep synthetic procedures. A representative example has been demonstrated that luminescent TCNB-based CT cocrystals (TCNB = 1,2,4,5-tetracyanobenzene) can be used to achieve two-color-emitting microdumbbells by a simple two-step seeded growth method.[15] These CT cocrystals were formed readily by slightly tuning the types of π-conjugated electron donors, which makes it possible to form the multi-color-emitting barcodes. On the basis of the structural understanding of the two-component CT cocrystals, more complex organic topological configurations could be designed and achieved by using preformed heterostructured materials rather than pure CT crystals as seeds, providing a rational design strategy for precise control on the assembly of multi-layer luminescent organic heterojunctions.

Herein, three luminescent TCNB-based CT cocrystals covering the emission colors of blue, green and orange were first synthesized via a simple solution-phase coassembly route following the previous synthetic procedures.[15] All three CT crystals display highly similar molecular packing because the π-conjugated molecules with a slight structural difference were used as electron donors, providing a possibility to integrate them into a heterostructured configuration through a process of solution epitaxial growth.[21] By applying a blue- and green-emitting CT microrod as a seed, two dual-color-emitting

[a] *Department of Applied Biology and Chemical Technology, The Hong Kong Polytechnic University, 999077, Hong Kong (China).*
**W.-Y. Wong E-mail: wai-yeung.wong@polyu.edu.hk*
[b] *Department of Chemistry, Institute of Molecular Functional Materials, Hong Kong Baptist University, 999077, Hong Kong (China)*

core-shell luminescent heterojunctions were achieved through a stepwise seeded-growth method. Moreover, the resultant core-shell microrods can be further applied as seeds to construct four more complex multi-color-emitting heterojunctions based on the same growth mechanism via solution epitaxy. The present rational construction of core-shell heterostructured materials was realized depending on perfect lattice matching of different CT crystals, offering a new sight to understand the effect of the structural relationship on the topological configurations.

## 2. Results and Discussion

### 2.1. Single-crystalline CT microrods composed of carbazole-type molecules and TCNB

We choose luminescent organic donor-acceptor (D-A) systems as the model materials to study the possibility of formation of multi-shell organic heterostructured materials. Typically, TCNB acts as the acceptor, whereas dibenzothiophene, fluorene and carbazole serve as the donors to synthesize three structurally similar CT compounds. In order to obtain crystalline one-dimensional (1D) CT assemblies, an etching assisted CT-induced assembly method was developed by adding a CT solution in THF to an ethanol/water mixture, as reported previously.[15] Instead of forming hollow tubes, three solid CT microrods including dibenzothiophene-TCNB (S-TCNB), fluorene-TCNB (C-TCNB), and carbazole-TCNB (N-TCNB) (Figure 1a) were achieved due to the high concentration of CT component and the high content of water in the THF/ethanol/$H_2O$ mixture. As shown in Figure 1b-d, scanning electron microscopy (SEM) results reveal that all of the three rod-like CT structures have a rectangular cross-section with a diameter of several micrometers, and a length of tens of micrometers. The corresponding transmission electron microscopy (TEM) images (Figure 1e-g) also confirm the formation of highly crystalline CT microrods. Even after storing them in the preparative solutions for two days, the CT microrods almost kept their initial morphologies.

The powder X-ray diffraction (XRD) tests of the three CT microrods were also performed to reveal their molecular packing (Figure 2a). Obviously, the XRD patterns are almost identical, indicating all of CT crystals have similar crystal structures. Thus, the slight structural differences of π-conjugated donors enable highly similar molecular packing of the resulting CT crystals as well as their structural consistency which have also been confirmed in their single crystal data (Figure 2g-i). These CT single crystals adopt π-π stacking mode in which the donor carbazolyl-type molecules and acceptor TCNB are nearly planar while being stacked one by one with basically the same interplanar spacing of 3.510 Å for S-TCNB, 3.493 Å for C-TCNB and 3.458 Å for N-TCNB with a very slight decline. Actually, the subsequently formed single-, double- and multi-layer core-shell microstructures all share nearly the same patterns due to the high similarity of these assembled supramolecular sub-units (see Figure S1 in Supporting Information). When excited by a UV lamp (365 nm), S-TCNB, C-TCNB, and N-TCNB microrods deposited on quartz substrates display uniform and strong blue, green and orange light. Their corresponding steady-state photoluminescence (PL) spectra were further studied and the broad PL bands of the three TCNB-based CT microrods appear at around 490, 540 and 590 nm (Figure 2b), respectively. In addition, the fluorescence microscopy images of these CT complexes reveal their emission colors ranging from blue through green to orange visually (Figure 2d-f). Solid-state absorption spectra of S-TCNB, C-TCNB and N-TCNB microrods were also measured for investigating the energy band gap of three CT complexes (Figure 2c). It is quite interesting that the slight structural differences of S-TCNB, C-TCNB, and N-TCNB can lead to such dramatic differences in the photophysical performances. That is, the emission and absorption properties of three TCNB-based CT microrods can be easily tailored via simply varying the electron-donating abilities of the donors. As reported previously,[22,23,24,25] the band gap between the frontier molecular orbitals for a CT cocrystal complex is redefined by the HOMO of a donor and the LUMO of an acceptor, resulting in a narrow band gap that is closely associated with the optoelectronic or/and photophysical property (Figure 3a).[24,25] Particularly, combined with the HOMO/LUMO energy levels of dibenzothiophene (-5.82/-0.95 eV),[26] fluorene (-5.76/-0.77 eV),[27,28] carbazole (-5.52/-0.62 eV)[29] and TCNB (-7.71/-3.89 eV) (Figure 3b),[30] the CT degrees of cocrystal complex are able to be deduced and compared by the electronic coupling between the HOMO of the carbazole-type molecules and the LUMO of the TCNB, that is, S–TCNB < C–TCNB < N–TCNB, which is directly related to the absorption property originating from the intermolecular CT state and is also consistent with the red-shifted emission wavelengths of three TCNB-based CT cocrystals. So far, the highly similar crystal structures and physicochemical properties of the TCNB-based CT crystals give us the possibility to construct organic heterojunctions by means of the epitaxy strategy. Besides, their obviously different luminescent colors could be exploited to recognize the composition of each domain of the heterostructured materials.[15]

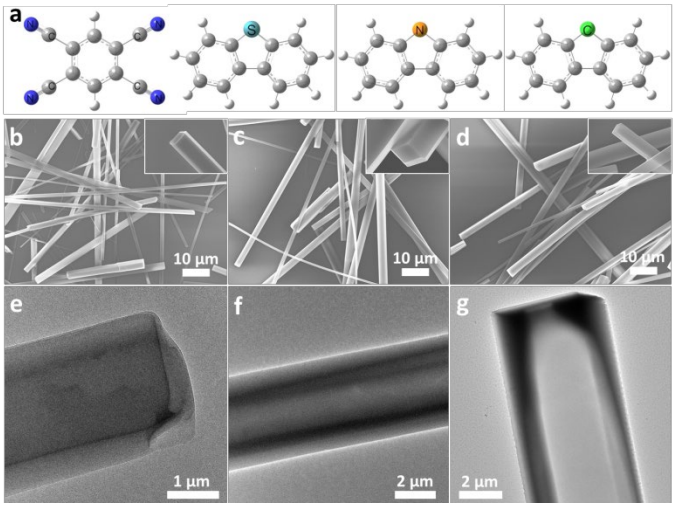


**Figure 1.** a. Schematic showing the molecular structures of 1,2,4,5-tetracyanobenzene (TCNB), dibenzothiophene (S), fluorene (C) and carbazole (N); b-d. SEM images of S-TCNB, C-TCNB and N-TCNB microrods with the SEM images of the corresponding transversal surfaces at the upper right corner; e-g. The TEM images of S-TCNB, C-TCNB and N-TCNB microrods, respectively.

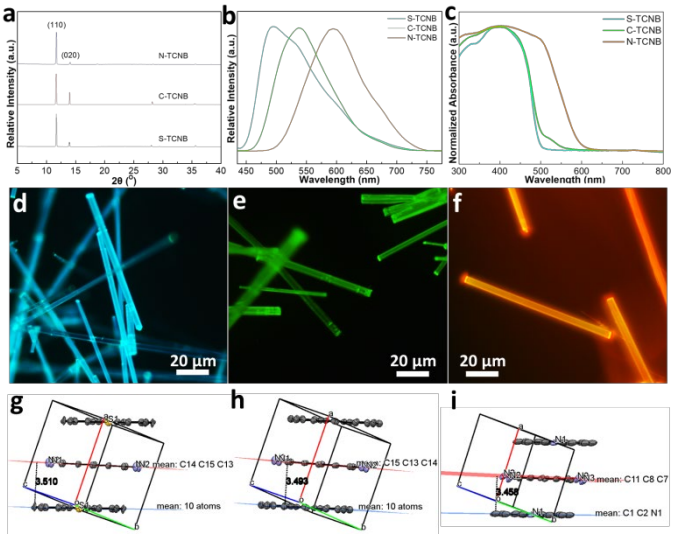


**Figure 2.** a. Powder XRD patterns of S-TCNB, C-TCNB and N-TCNB microrods. b. Photoluminescence (PL) spectra of S-TCNB, C-TCNB and N-TCNB microrods. c. Solid-state absorption spectra of S-TCNB, C-TCNB and N-TCNB microrods. d-f. Fluorescence microscopy images of S-TCNB, C-TCNB, and N-TCNB microrods upon excitation with UV light. g-i. Molecular packing modes in sigle crystals S-TCNB, C-TCNB, and N-TCNB.

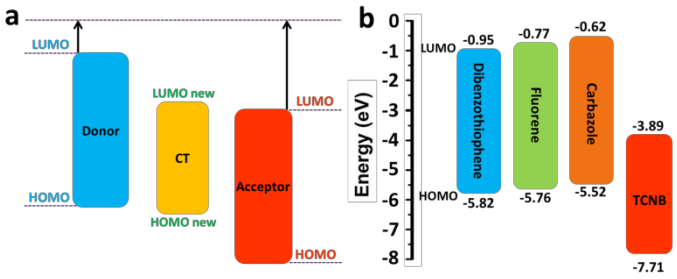


**Figure 3.** a. HOMO-LUMO engineering, schematic diagram of orbital energy levels and band positions of donor (blue), acceptor (red) and CT cocrystal (yellow). b. Energy-level diagrams of dibenzothiophene, fluorene, carbazole and TCNB.

### 2.2. Single-layer CT core-shell structures: S-TCNB@N-TCNB and C-TCNB@N-TCNB

To examine our hypothesis, a stepwise seeded-growth approach was designed to synthesize single- and multi-layer core-shell microstructures. For single-layer core-shell structures, one CT crystal was selected as a seed and another CT crystal as the second growth component. For multi-layer core-shell structures, the above-mentioned core-shell structures were repeatedly used as a seed and one specific CT crystal as the subsequent growing unit. Importantly, multi-layer core-shell structures even up to three-layer shells can be formed by rationally pairing different CT constituent materials. To reduce the disassembly process in the formation of single- and multi-layer core-shell structures, one preformed CT microrod seed was first dispersed in an ethanol/water mixture with an appropriate volume ratio, and then another CT solution in THF was rapidly mixed with the seed suspension. The solvent-exchange process greatly reduces the solubility of the second growing component, triggering its selective deposition onto the surface of the starting seed, which can be regarded as involving a process of solution epitaxial growth.[21]

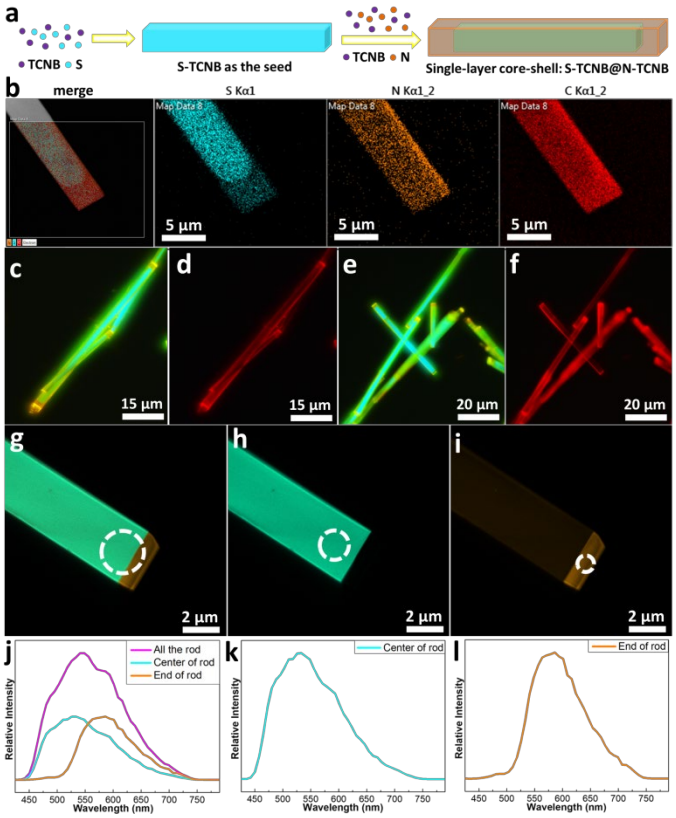


**Figure 4.** a. Schematic illustration of the synthetic procedure of single-layer core-shell microrods by using a stepwise seeded growth method. b. TEM EDS elemental mapping of S-TCNB@N-TCNB. c-f. Fluorescence microscopy images of S-TCNB@N-TCNB excited by UV and green light, respectively. g-l. Laser confocal fluorescence microscopy (LCFM) photographs collected from the blue (h), orange (i) light wavelength range and their overlay (g) upon the excitation with blue light ($\lambda_{ex}$ = 405 nm) besides their micro-area PL spectra (j-l) recorded from the selected areas that are marked in black circles on the S-TCNB@N-TCNB.

For constructing single-layer core-shell heterostructured microrods, blue-emitting S-TCNB and orange-emitting N-TCNB crystals were specially selected as a seed and growing unit, respectively (Figure 4a). Specifically, the seed suspension was achieved by dispersion of S-TCNB microrods into an appropriate ethanol/water mixture. Upon mixing the suspension with N-TCNB solution in THF, N-TCNB serves as the shell layer to form S-TCNB@N-TCNB core-shell structures. TEM EDS elemental mapping of S-TCNB@N-TCNB microrod proves the formation of core-shell structure, in which the carbon (C) and nitrogen (N) cover the whole area of heterojunction, sulphur (S) is concentrated on the core area of heterojunction (Figure 4b). The EDS spectra of elemental line scan on prepared S-TCNB@N-TCNB show the consistent result, the carbon (C) and nitrogen (N) show their signals simultaneously as the line scanned to the boundary of heterojunction, then at the interface of heterojunction, sulphur (S) started to show its signal (Figure S5). Fluorescence microscopy tests were performed to examine the configuration because different layers can be distinguished by their different emission colors. Figure

4c-f shows the corresponding images excited by UV and green light, respectively. As expected, a yellow-emitting thin layer is deposited onto the surface of a blue-emitting microrod upon excitation with UV light (Figure 4c, e). When the excitation light was converted into a green light, the inner core almost becomes non-emissive, while the outer layer exhibits a strong red light (Figure 4d, f). Thus it is clearly confirmed that N-TCNB layer is uniformly coated onto the surface of S-TCNB microrods, forming S-TCNB@N-TCNB core-shell structures. Laser confocal fluorescence microscopy (LCFM) test was also carried out to further reveal that N-TCNB layer would preferentially grow along the 1D direction rather than the intersecting axes (Figure 4g-i). We thereby inferred that a larger amount of exposed acceptor (TCNB) or/and donor (dibenzothiophene) molecules at the tips rather than on the walls of S-TCNB would offer more possibilities for the selective deposition of N-TCNB, as described previously.[15] The corresponding micro-area PL spectrum of S-TCNB@N-TCNB core-shell structures at the core-shell junction shows a PL peak at 490 nm at the short-wavelength range, a PL peak at 540 nm at the median-wavelength range and a PL peak at 590 nm at the long-wavelength range. When compared to the PL peak of the core-shell structure at the tip (590 nm), it can be clearly confirmed that the PL peaks at 490 nm should be derived from the inner S-TCNB core, the PL peak at 590 nm should be originated from the outer N-TCNB layer (Figure 4j-l), while the PL peak at 540 nm is the superposition of two spectral shoulders. The above results further support the formation of S-TCNB@N-TCNB core-shell structure. Furthermore, green-emitting C-TCNB can also be used as a seed to afford the formation of C-TCNB@N-TCNB core-shell structure (Figure S8).

**2.3. Two-layer CT core-shell structures: S-TCNB@N-TCNB@C-TCNB and C-TCNB@N-TCNB@S-TCNB**

Inspired by the above result, we wondered whether S-TCNB@N-TCNB core-shell structure can be further used as a seed to construct a more complex two-layer S-TCNB@N-TCNB@C-TCNB core-shell configuration following the same growth mechanism, in which C-TCNB serves as another growth component. The present synthetic procedures were almost identical to the case of S-TCNB@N-TCNB core-shell structure except for the alternation of the seed (Figure 5a). The formation of core-shell structure is proved by TEM EDS elemental mapping of S-TCNB@N-TCNB@C-TCNB microrod, in which the carbon (C) covers the whole area of heterojunction, nitrogen (N) and sulphur (S) are concentrated on the specific core areas of heterojunction (Figure 4b). The EDS spectra of elemental line scan on S-TCNB@N-TCNB@C-TCNB exhibit the consistent result, the carbon (C) was detected since the scan line arrived at the boundary of heterojunction, then nitrogen (N) was detected started from the outside interface, at last sulphur (S) was detected started from the inside interface of heterojunction (Figure S5). The EDS results well support the fabrication of CT core-shell structures. From the fluorescence microscopy results shown in Figure 5c and e, we can see that orange-emitting N-TCNB layer is coated by a thin green-emitting C-TCNB layer when excited by UV light, giving a two-layer S-TCNB@N-TCNB@C-TCNB core-shell structure. Upon the excitation with a green light, two separate junctions with the obvious interface at the tip part were clearly observed, indicating the formation of a two-layer core-shell structure as well (Figure 5d, f). In some cases, the innermost blue-emitting core S-TCNB can also be observed, as recognized via the typical magnified images of two-layer core-shell structure. Laser confocal fluorescence microscopy (LCFM) results further demonstrate that a tip of the two-layer core-shell structure involves two junctions at the core-shell interface (Figure 5g-j). The corresponding micro-area PL spectrum shows that the PL band of the position in Figure 5j at 540 nm corresponds to C-TCNB. While the position in Figure 5i has a PL band at 575 nm, which corresponds to both C-TCNB and N-CTNB. Obviously, the PL bands of the positions in Figure 5g and h have almost the same spectral profiles, indicating that both of them were composed of all three constituent materials, the only difference is the peak intensity of 490 nm corresponding to S-TCNB in Figure 5l is slightly higher than Figure 5k, meaning that the position in the center of core-shell rod contains more S-TCNB composition than the other positions of the rod (Figure 5k-n). The above results clearly confirm the formation of a S-TCNB@N-TCNB@C-TCNB core-shell structure with triple-color-emitting property. Similarly, C-TCNB@N-TCNB could also be used as a seed to afford the formation of C-TCNB@N-TCNB@S-TCNB core-shell structure (Figure S9).

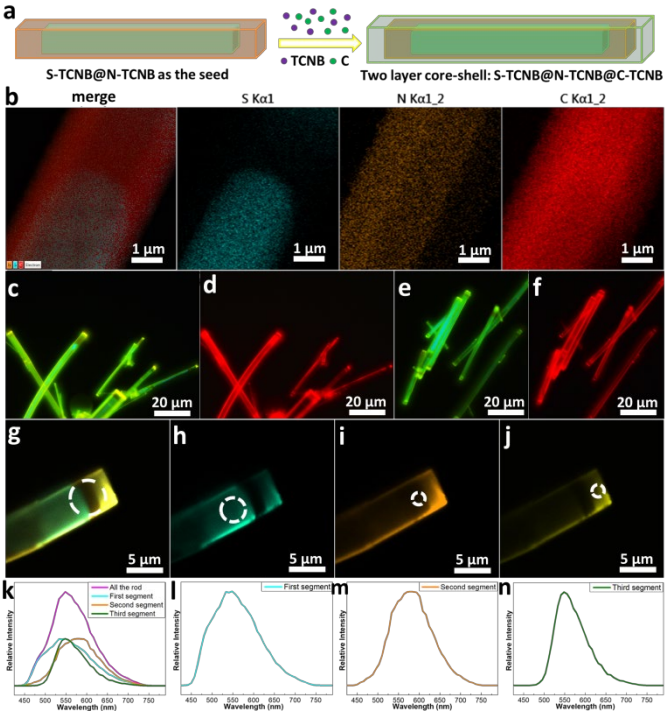


**Figure 5.** a. Schematic illustration of the synthetic procedure of two-layer core-shell microrods by using a stepwise seeded growth method. b. TEM EDS elemental mapping of S-TCNB@N-TCNB@C-TCNB. c-f. Fluorescence microscopy images of S-TCNB@N-TCNB@C-TCNB rods excited by UV and green light, respectively. g-n. LCFM photographs collected from the blue (h), orange (i), yellow (j) light wavelength range and their overlay (g) upon the excitation with blue light ($\lambda_{ex}$ = 405 nm) besides their micro-area PL spectra (k-n) recorded from the selected areas that are marked in black circles on the S-TCNB@N-TCNB@C-TCNB rod.

**2.4. Three-layer CT core-shell structures: S-TCNB@N-TCNB@C-TCNB@N-TCNB and C-TCNB@N-TCNB@S-TCNB@N-TCNB**

So far, we have successfully prepared the one-layer and two-layer core-shell strucutures composed of TCNB-based CT co-crystals. In order to prove these three CT co-crystals can simply grow on each other based on their perfect lattice matching, next, we continue to devise and construct a three-layer core-shell structure S-TCNB@N-TCNB@C-TCNB@N-TCNB by using the S-TCNB@N-TCNB@C-TCNB heterostructured microrod as a seed and N-TCNB as the growing unit (Figure 6a). Similar to the case of S-TCNB@N-TCNB@C-TCNB core-shell structure, the above three-layer core-shell structure could also be synthesized by a stepwise seed-induced solution epitaxy method. As expected, each tip of the 1D microstructure has three junctions with different colors when excited by UV light, as the fluorescence microscopy results shown in Figure 6b, d and f. Upon converting the excitation light to a green light, two orange-emitting junctions would become red, while the blue- and green-emitting junctions would become non-emissive (Figure 6c, e and g). Hence, the multi-junction structure can be regarded as a multiple core-shell structure. The sequence of each component from inner to outer layer in the core-shell structure should be S-TCNB@N-TCNB@C-TCNB@N-TCNB. Furthermore, C-TCNB@N-TCNB@S-TCNB could be used as a seed as well to afford the fabrication of C-TCNB@N-TCNB@S-TCNB@N-TCNB core-shell structure as well (Figure 6h). With the same constituent CT complex composition but different organized sequence, their final multi-layer pattern formed and emitting color are almost identical to those of the S-TCNB@N-TCNB@C-TCNB@N-TCNB (Figure 6i-n).

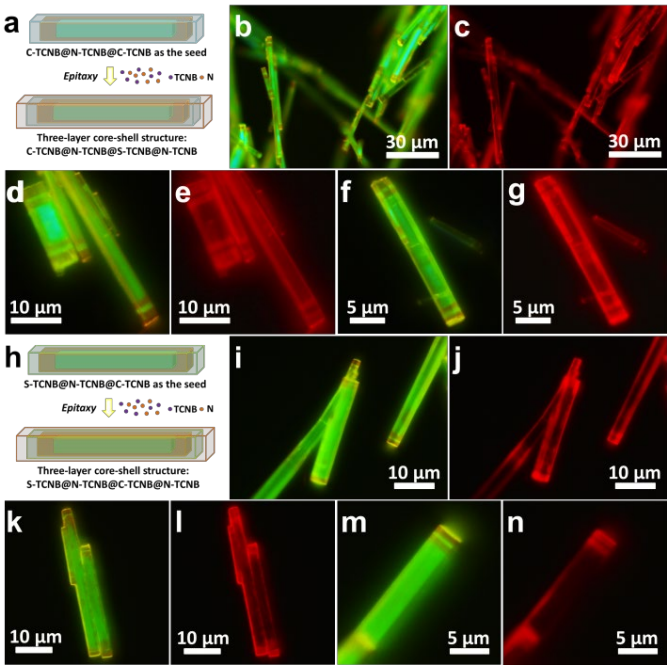


**Figure 6.** a. Schematic illustration of the prepared procedure using the stepwise seed-reduced growth method to prepare the three-layer core-shell microrods S-TCNB@N-TCNB@C-TCNB@N-TCNB. b-g. Fluorescence microscopy images of the corresponding three-layer core-shell rods excited by UV and green light from low to high magnification (b-c at a view of the whole rods, d-e at a view of the rod-tip, f-g at a view of the single rod). h. Schematic illustration of the prepared procedure using the stepwise seed-reduced growth method to prepare the three-layer core-shell microrods C-TCNB@N-TCNB@S-TCNB@N-TCNB. i-n. Fluorescence microscopy images of the corresponding three-layer core-shell rods excited by UV and green light from low to high magnification.

## 3. Growth mechanism

Growth mechanism of the second CT unit growing on the preformed crystalline CT seed to form multi-layer organic core-shell structures was explicated by structural analysis of the three crystals, epitaxy process besides the surface-interface energy balance as well.[21,31,32] It was reported that TCNB-based CT crystals possessing π-π stacking structure in which the two constituent molecules are nearly planar and stacked by turn along the c axis.[15,33] This is why most of our prepared CT complexes show 1D orientation, and result in a larger amount of donor and/or acceptor molecules exposed at the end facets, which would guide the selective nucleation of next binary complexes on account of the strong CT interaction between the carbazole-type donor molecules and the TCNB acceptor. All the unit cells of three CT cocrystals have almost identical lattice parameters along *a*, *b* and *c* axes (*a* = 7.16 Å, *b* = 7.82 Å, *c* = 7.92 Å for dibenzothiophene-TCNB, *a* = 7.18 Å, *b* = 7.78 Å, *c* = 7.94 Å for fluorene-TCNB and *a* = 7.01 Å, *b* = 7.86 Å, *c* = 7.86 Å for carbazole-TCNB, Figure S10 and Table S1) as well as identical lattice angles along *α*, *β* and *γ* directions (*α* = 72.92°, *β* = 86.08°, *γ* = 89.28° for dibenzothiophene-TCNB, *α* = 73.80°, *β* = 83.80°, *γ* = 88.45° for fluorene-TCNB and *α* = 73.65°, *β* = 84.33°, *γ* = 88.87° for carbazole-TCNB, Figure S10 and Table S1), hence formation of a continuous as well as uniform core-shell geometry would be easy and rational in a prescriptive pattern. Furthermore, the crystal data can also support our interpretation about the process of solution epitaxial growth because of the nearly same crystallographic parameters of growing unit and seed unit. As soon as the new solution of growing unit is added, the original seed unit formed is etched very slightly by the new solution. Then subsequent epitaxial growth from the next substantially similar complex results in a larger heterogeneous architecture. Consequently, the epitaxial growth would basically remain the original form of the microstructure, and thus this explains what we fabricated is the core-shell heterostructure rather than the other shape-like heterostructure (Figure 7). Meanwhile, the surface-interface energy balance analysis also reveals that the epitaxy preferentially favors the next TCNB-based CT complex nucleation at the end facets which leads to selective deposition along the 1D direction rather than the intersecting axes, as it could reduce the unstable nature or high energy of the former two-component CT complex facets, as in the case that we reported before.[15] Regarding the applications of this kind of CT materials, we are currently using these CT complexes to dope with each other to build a light-harvesting system for realizing tunable emission,[25] even for the generation of white-light emission (WLE).[30,33] It has also been known that the TCNB-based CT complexes possess the nature of ambipolar charge transport,[22,25] high fluorescence

quantum yield, good optical waveguide as well as two-photon emission properties.[34] Besides our designed and controllable assembly of different CT constituents to form various tactic multi-color-emitting heterostructures, here we offer a facile and efficient way to prepare programmable encoding organic barcodes with potential photofunctional application.

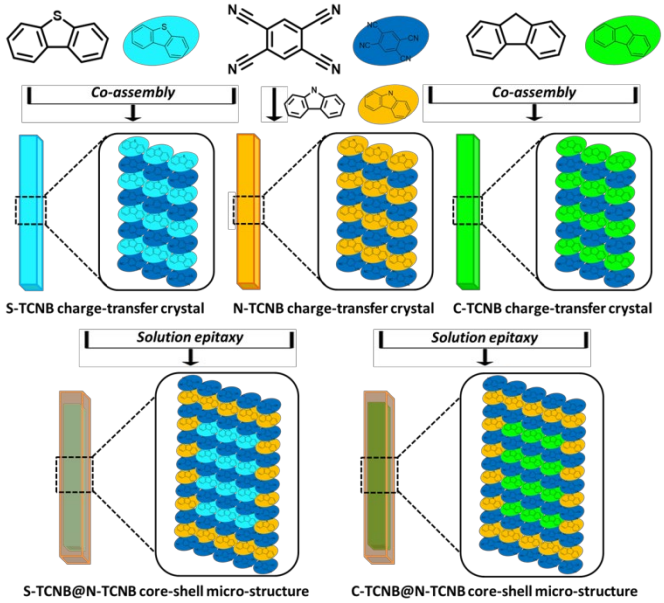


**Figure 7.** Schematic illustration of the possible formation process and mechanism for supramolecular core-shell heterostructures S-TCNB@N-TCNB and C-TCNB@N-TCNB in two-dimensional growing directions (In three-dimensional growing directions, they should be the capsulated structures, and TCNB-based CT crystals possess π-π stacking inner structure in which the two constituent molecules are nearly planar and stacked by turn along one axis).

## Conclusions

Three CT cocrystal microrods S-TCNB, C-TCNB and N-TCNB with a wide emission color ranging from blue through green to orange were first synthesized by a simple solution coassembly method. Importantly, a stepwise seed-induced solution epitaxy approach has been successfully developed to construct single- and multi-layer core-shell microstructures. A CT cocrystal can be employed as a seed and another CT cocrystal serves as the second growth unit to prepare a single-layer core-shell micro-structure, which can also be repeatedly applied as a seed to construct more complex multi-layer core-shell structures. This successful example on the precisely controllable formation of supramolecular multi-color-emitting core-shell heterojunctions opens a new door towards constructing more sophisticated and functional organic heterogeneous materials.

## Conflicts of interest

The authors declare no competing financial interest.

## Acknowledgements

W.-Y.W. acknowledges the financial support from the Hong Kong Research Grants Council (PolyU153062/18P), Areas of Excellence Scheme of HKSAR (AoE/P-03/08), The Hong Kong Polytechnic University (1-ZE1C) and Ms Clarea Au for the Endowed Professorship in Energy (847S).

## Notes and references

1 F. Ebisawa, T. Kurokawa, S. Nara, *J. Appl. Phys.* 1983, **54**, 3255–3259.
2 K. Kudo, M. Yamashina, T. Moriizumi, *Jpn. J. Appl. Phys.* 1984, **23**, 130.
3 A. Tsumura, H. Koezuka, T. Ando, *Appl. Phys. Lett.* 1986, **49**, 1210–1212.
4 F. Garnier, R. Hajlaoui, A. Yassar, P. Srivastava, *Science* 1994, **265**, 1684–1686.
5 C. D. Dimitrakopoulos, P. R. L. Malenfant, *Adv. Mater.* 2002, **14**, 99–117.
6 C. W. Tang, S. A. VanSlyke, *Appl. Phys. Lett.* 1987, **51**, 913–915.
7 C. Adachi, W. Tokito, T. Tsutsui, S. Saito, *Jpn. J. Appl. Phys.* 1988, **27**, 269–271.
8 M. A. Baldo, D. F. O'Brien, Y. You, A. Shoustikov, S. Sibley, M. E. Thompson, S. R. Forrest. *Nature* 1998, **395**, 151–154.
9 P. Peumans, S. R. Forrest, *Appl. Phys. Lett.* 2001, **79**, 126–128.
10 P. Peumans, S. Uchida, Forrest, S. R. *Nature* 2003, **425**, 158–162.
11 A. J. Heeger, *Adv. Mater.* 2014, **26**, 10–28.
12 Y. Huang, E. J. Kramer, A. J. Heeger, G. C. Bazan, *Chem. Rev.* 2014, **114**, 7006–7043.
13 S. R. Forrest, *Nature* 2004, **428**, 911–918.
14 Y. J. Zhang, H. L. Dong, Q. X. Tang, S. Ferdous, F. Liu, W. P. Hu, A. L. Briseno, *J. Am. Chem. Soc.* 2010, **132**, 11580–11584.
15 Y. L. Lei, L. S. Liao, S. T. Lee, *J. Am. Chem. Soc.* 2013, **135**, 3744–3747.
16 Y. Lei, Q. Liao, H. Fu, J. Yao, *J. Am. Chem. Soc.* 2010, **132**, 1742–1743.
17 M.-J. Sun, Y. Liu, Y. Yan, R. Li, Q. Shi, Y. S. Zhao, Y.-W. Zhong, J. Yao, *J. Am. Chem. Soc.* 2018, **140**, 4269–4278.
18 J. Zhang, H. Geng, T. S. Virk, Y. Zhao, J. H. Tan, C. A. Di, W. Xu, K. Singh, W. P. Hu, Z. G. Shuai, Y. Q. Liu, D. B. Zhu, *Adv. Mater.* 2012, **24**, 2603–2607.
19 J. Zhang, J. H. Tan, Z. Y. Ma, W. Xu, G. Y. Zhao, H. Geng, C. A. Di, W. P. Hu, Z. G. Shuai, K. Singh, D. B. Zhu. *J. Am. Chem. Soc.* 2013, **135**, 558–561.
20 W. Zhang, W. S. Jing, T. Fukushima, A. Saeki, S. Seki, T. Aida, *Science* 2011, **334**, 340–343.
21 C. Xu, P. He, J. Liu, A. Cui, H. Dong, Y. Zhen, W. Chen, W. Hu, *Angew. Chem. Int. Ed.* 2016, **55**, 9519-9523.
22 H. D. Wu, F. X. Wang, M. Zhang, G. B. Pan, *Nanoscale*, 2015, **7**, 12839-12842.
23 M. Schwarze, W. Tress, B. Beyer, F. Gao, R. Scholz, C. Poelking, K. Ortstein, A. A. Günther, D. Kasemann, D. Andrienko, K. Leo, *Science*, 2016, **352**, 1446-1449.
24 H. Jiang, P. Hu, J. Ye, K. K. Zhang, Y. Long, W. Hu, C. Kloc, *J. Mater. Chem. C* 2018, **6**, 1884-1902.
25 L. Sun, W. Zhu, F. Yang, B. Li, X. Ren, X. Zhang, W. Hu, *Phys. Chem. Chem. Phys.* 2018, **20**, 6009-6023.
26 C. S. Oh, H. L. Lee, W. P. Hong, J. Y. Lee, *J. Mater. Chem. C*, 2019, **7**, 7643.
27 X. Y. Liu, F. Liang, L. Ding, S. C. Dong, Q. Li, L. S. Cui, Z. Q. Jiang, H. Chen, L. S. Liao, *J. Mater. Chem. C*, 2015, **3**, 9053-9056.
28 E. Bindewald, R. Lorenz, O. Hübner, D. Brox, D. P. Herten, E. Kaifer, H. J. Himmel, *Dalton Trans. 2015,* **44***, 3467–3485*.

29 A. Quashie, *J. Nanosci. Nanotech. Applic.* 2018, **2**, 1-12.
30 Y. Sun, Y. Lei, L. Liao, W. Hu, Angew. Chem. 2017, **129**, 10488 –10492.
31 L. Carbonea, P. D. Cozzolia, *Nano Today* 2010, **5**, 449–493.
32 R. Buonsanti, V. Grillo, E. Carlino, C. Giannini, F. Gozzo, M. Garcia-Hernandez, M. A. Garcia, R. Cingolani, P. D. Cozzoli, *J. Am. Chem. Soc.* 2010, **132**, 2437–2464.
33 Y. L. Lei, Y. Jin, D. Y. Zhou, W. Gu, X. B. Shi, L. S. Liao, S. T. Lee, *Adv. Mater.* 2012, **24**, 5345–5351.
34 X. Fang, X. Yang, D. Yan, *J. Mater. Chem. C* 2017, **5**, 1632–1637.